Applied Catalysis B: Environmental 113–114 (2012) 192–200

Contents lists available at SciVerse ScienceDirect

Applied Catalysis B: Environmental

journal homepage: www.elsevier.com/locate/apcatb

Simultaneous production of H_2 and C_2 hydrocarbons by gas phase electrocatalysis

A. Caravaca, A. de Lucas-Consuegra*, J. González-Cobos, J.L. Valverde, F. Dorado

Departamento de Ingeniería Química, Facultad de Ciencias Químicas, Universidad de Castilla-La Mancha, Avenida Camilo José Cela 12, 13005 Ciudad Real, Spain

ARTICLE INFO

Article history:
Received 19 September 2011
Received in revised form
16 November 2011
Accepted 18 November 2011
Available online 26 November 2011

Keywords:
H_2 production
Oxidative coupling of methane
C_2 hydrocarbons
Gas phase electrocatalysis
Steam electrolysis

ABSTRACT

This study reports, for the first time in literature, the possibility of simultaneously producing H_2 and C_{2s} hydrocarbons by using an anionic single chamber solid electrolyte cell of Pt/YSZ/Ag (working/solid electrolyte/counter) tested under a humidified CH_4 atmosphere (no direct O_2 feeding gas to the reactor). Hydrogen was mainly produced in the Pt working electrode under application of negative polarizations by a steam electrolysis process ($H_2O + 2e^- \rightarrow H_2 + O^{2-}$). Simultaneously, the produced O^{2-} ions were electrochemically pumped to the Ag counter electrode, leading to the production of C_{2s} hydrocarbons (ethane and ethylene), via oxidative coupling of CH_4 ($CH_4 + O^{2-} \rightarrow C_2H_4 + C_2H_6 + 2e^-$). The influence of the applied current, reaction temperature and feeding composition on the electrocatalytic performance of the cell was evaluated for both processes. It was found that the possibility of controlling the rate of O^{2-} supply allows to control and optimize the production rate of the desired compounds (H_2 and C_{2s}) at varying the reaction conditions. In addition, the stability of the cell for long polarization times has been demonstrated under the optimal conditions for the production of both compounds.

1. Introduction

As the major constituent of natural gas, methane is a raw material of great importance; however, two factors limit its use. The first one is that transporting natural gas or liquefied natural gas is not economical and hence it is highly desirable to convert methane into transportable raw materials or products. The second is that methane is a refractory molecule, very difficult to convert to upgraded products. Hence, two kinds of products of great importance can be obtained from methane: hydrogen and C_2 hydrocarbons (e.g., ethylene). The production of hydrogen is attracting great interest as a future clean fuel for combustion engines and fuel cells [1]. Nowadays, different technologies have been developed for H_2 production from methane, which mainly involves catalytic processes such as: steam reforming, partial oxidation or autothermal reforming [2–8]. On the other hand the conversion of methane into higher hydrocarbons (ethane and ethylene –C_{2s}–) has also significant importance, being the oxidative coupling process (OCM) one of the most important route [9]. A lot of research work on the OCM process has been made since the pioneering work of Keller and Bhasin in 1982 [10]. However, there are difficulties in the direct conversion of methane because the heterogeneous catalytic oxidation usually results in complete combustion products, carbon dioxide and water, with limited selectivity to C_{2s} products [11]. Hence one of the main drawbacks of this process is the typical low concentration of ethylene in the stream, which makes the required separation uneconomical. Thus, different improvements have been introduced to increase the overall efficiency of the process such as the distribution of O_2 in the feed, additional conversion of the produced ethylene into less volatile products or the use of counter current moving-bed chromatographic separation reactor [12]. However, until now a definitive configuration has not been found for the industrial application of this process, and hence sustained R&D efforts are essential to make the OCM process commercially feasible.

In this work we propose a novel improvement in the OCM process, which can increase its economical feasibility, by integrating the simultaneous co-production of another product of great economic interest, H_2, through the use of a solid electrolyte membrane reactor (SEMR). A SEMR consists mainly of a ceramic solid electrolyte membrane (e.g., O^{2-} or H^+ conductor in most cases), in which two porous metal or metal oxide electrodes are deposited on both sides of the membrane. These kinds of configurations allow to electrochemically supply one of the reactives (e.g., O^{2-} for the oxidative coupling reaction) by a Faradaic operation [13]. These kinds of configurations have already been used in the OCM reaction by using both: O^{2-} and H^+ conducting membranes and have been described in detail in excellent reviews made by the group of Prof. Stoukides [13–16]. The option of using this kind of reactors presents several advantages such as: enhanced catalytic activity and selectivity, better process integration, reduced feedstock and easy reaction rate control [17]. In addition, there are combined possibilities of electrochemical enhancement of C_2 selectivity, simultaneous generation of electrical power, and in general,

* Corresponding author. Tel.: +34 926295300; fax: +34 926295437.
E-mail address: Antonio.Lconsuegra@uclm.es (A. de Lucas-Consuegra).

0926-3373/$ – see front matter © 2011 Elsevier B.V. All rights reserved.
doi:10.1016/j.apcatb.2011.11.037

more control over the reaction pathway. For instance, Otsuka et al. [18] first studied the OCM reaction in SEMR with Ag or Ag/Bi_2O_3 applied on yttria-stabilized zirconia (YSZ) in 1985. The results showed that oxygen supplied by YSZ (by electrochemical pumping of O^{2-} ions to the Ag electrode) was more active than gas-phase supplied oxygen. Two years later [19], they studied the same system with LiCl/NiO catalyst electrode. The C_{2s} selectivity could reach 92%. They concluded that O^{2-} pumping created active oxygen species for C_{2s} hydrocarbons on the LiCl/NiO. More recently, the group of Prof. Vayenas [20,21] has also reported the non-Faradaic electrochemical modification of the catalytic activity (NEMCA effect), which can dramatically enhance both: the rates and the C_{2s} selectivity of the OCM. Also, in a previous work [22] Jiang et al. studied the oxidative coupling reaction in a fuel cell type reactor. In this case, it was used as a novel gas recycle high temperature system, leading to ethylene yields up to 85%. These are only some examples of a great number of studies carried out on OCM reaction for the production of C_{2s} hydrocarbons by using O^{2-} conducting solid electrolyte membrane reactors [13–16]. However in all those previous studies, the O^{2-} reacting ions were electrochemically supplied to the active catalyst film from the O_2 coming from the gas phase or the air, and hence, the C_{2s} hydrocarbons were the unique valuable products.

In this work we present a radically novel configuration for upgrading methane towards the simultaneous production of H_2 and C_{2s}. In this sense, a single chamber solid electrolyte cell has been developed (Pt/YSZ/Ag), where both active electrodes Pt and Ag were exposed to the same reaction atmosphere (a mixture of CH_4 and H_2O). In this case, no O_2 was directly supplied from the gas phase for the OCM, and hence, the active O^{2-} ions for the OCM reaction were in situ electrochemically produced from H_2O through a steam electrolysis process ($H_2O + 2e^- \rightarrow H_2 + O^{2-}$). This configuration would reduce the cost of the process since no pure O_2 is required for feeding the reactor and at the same time it would allow to produce H_2. Hence, by the same applied electrical current, both kinds of products (H_2 and C_{2s}) could be simultaneously obtained, which may be satisfactory for an economically feasible production of ethylene, and hence for the further implementation of this process. Additionally, two other important advantages can be addressed to the proposed system configuration. Firstly, the possibility of combining an exothermic reaction (oxidative coupling) with an endothermic one (steam electrolysis) by heat transfer of all the gas components in the well mixed single chamber reactor configuration. The second one is that at the same time the oxidative coupling of methane reaction could act as a depolarizing agent in the single chamber steam electrolysis cell, increasing its power efficiency and hence decreasing the electrical power input requirements through a natural gas assisted electrolysis cell NGASE [23]. Additionally, the use of a single chamber cell simplifies its further practical application to the existing catalytic process since it does not require reactants to be separated.

2. Experimental

2.1. Solid electrolyte cell preparation

The solid electrolyte cell consisted of a porous and continuous Pt thin film (geometric area of 2.01 cm^2) deposited on a side of a 19-mm-diameter, 1-mm-thick YSZ (yttria-stabilized zirconia) disc (Tosoh-Zirconia). Ag counter electrode (geometric area of 2.01 cm^2) and an Au reference electrode (geometric area of 0.1 cm^2), were deposited on the other side of the electrolyte. Firstly, both the Au (reference) and the Ag (counter) electrodes were deposited by application of thin coatings of Au (Gwent Electronic Materials) and Ag (Fuel Cell Materials) pastes, respectively, followed by two calcination steps, at 300 °C (2 h) and 850 °C (2 h). The final Ag loading was 10 mg Ag/cm^2. The selection of Ag as the active catalyst film for the OCM has been done due to the easy preparation method and the promising results obtained in previous studies in the oxidative coupling reaction [11,21]. Then, the Pt film was deposited, as described in detail elsewhere [23], by successive steps of deposition and thermal decomposition in two steps (550 °C for 1 h and 850 °C for 2 h, with a heating ramp of 5 °C/min) of a H_2PtCl_6 precursor solution over a mixture of 1/1 H_2O/2-propanol with a metal concentration of 0.1 M. The final Pt loading was 1.36 mg Pt/cm^2. The typical dispersion value for the paste prepared electrodes is below 1% [24], while for the impregnation prepared electrodes, it is normally around 3% [25]. The electrodes (working, counter and reference) were connected to the potentiostat-galvanostat Voltalab 21 (Radiometer Analytical). In this work all the experiments were carried out under galvanostatic imposition. Au was chosen as the reference electrode material because of its inertness for the explored reactions checked via blank experiments.

2.2. Catalytic activity measurements

The activity measurements were carried out in the experimental setup described in detail in a previous work [24]. It consisted of a single chamber solid electrolyte cell, with all the electrodes exposed to the same reaction atmosphere. The reaction gases (Praxair, Inc.) were certified standards of 10% CH_4/N_2 and N_2 (99.999% purity), which was used as the carrier gas. The gas flow was controlled by a set of calibrated mass flowmeters (Brooks 5850 E and 5850 S) while water was introduced to the feed stream by means of a saturator in order to achieve liquid–vapour equilibrium. The content of water in the reaction mixture was controlled by using the vapour pressure of H_2O at the temperature of the saturator (39 °C). All lines placed downstream from the saturator were heated above 100 °C to prevent condensation. The reactants were introduced into the reactor with the following concentrations: CH_4 (0.3–1.3%), H_2O (7%), N_2 balance, with an overall gas flow rate of 60 mL min^{-1}. All the catalytic experiments were carried out between 750 and 820 °C at atmospheric pressure. Reactant and product gases were analyzed with a micro gas-chromatograph (Varian CP-4900) equipped with two columns (Molsieve and Poraplot Q column) and two thermal conductivity detectors (TCD). The first column enabled the separation of H_2 and CO while the second column allowed separating CO_2, C_2H_4, C_2H_6 and H_2O. Before the analysis, the water contained in the effluent streams was trapped by a condenser at −2 °C. The main detectable products were C_2H_6, C_2H_4, CO_2, CO and H_2. The error in the carbon atom balance did not exceed 2%, which indicates no consistent loss of material, no significant formation of other oxygenated species and/or coking of the catalyst-electrodes. CH_4 conversion and C_2's selectivity and yield were calculated as follows:

$$CH_4 \ \text{conversion} = \frac{F^{\circ}_{CH_4} - F_{CH_4}}{F^{\circ}_{CH_4}} \times 100 \quad (1)$$

$$C_{2s} \ \text{selectivity} = 2 \times \frac{F_{C_2H_4} + F_{C_2H_6}}{F^{\circ}_{CH_4} - F_{CH_4}} \times 100 \quad (2)$$

$$C_{2s} \ \text{yield} = \frac{CH_4 \ \text{conversion} \times C_{2s} \ \text{selectivity}}{100} \quad (3)$$

On the other hand, in order to evaluate the efficiency of the single chamber steam electrolysis cell, an apparent Faradaic efficiency (Λ) was defined in order to relate the amount of experimentally measured H_2 leaving the reactor with the applied current:

$$\Lambda = \frac{r_{H_2} - r^0_{H_2}}{I/2F} \quad (4)$$

where r_{H_2} and $r^0_{H_2}$ were the hydrogen reaction rates under closed circuit and open circuit conditions, respectively, and F is the Faraday's constant.

3. Results and discussion

3.1. Influence of the applied current

In order to demonstrate the activity of both, the Pt (working) and the Ag (counter) electrodes for the proposed reactions, a galvanostatic transient experiment was carried out. It was performed by step changes in the applied current at a constant temperature of 750 °C under the following conditions: CH_4/H_2O: 1%/7%, with a total flow rate of 60 mL min^{-1} (N_2 balance). Fig. 1 depicts the response of the obtained products: H_2 (a), CO and CO_2 (b), as well as C_2H_4 and C_2H_6 (c) production rates vs. time under open circuit conditions (OCV from now on), and under the application of a positive (200 mA) and a negative current (−200 mA). In addition, Fig. 1a shows the variation of the free O_2 present in the reaction atmosphere, as will be described below. In first place, it can be observed the negligible activity of the electrochemical cell for both H_2 and C_{2s} production under open circuit potential conditions, i.e., no catalytic activity of both electrodes for a possible reforming process or coupling reaction towards the production of H_2 and C_{2s} under OCV was detected. Nevertheless, a strong increase in the reaction rates was observed during current impositions, mainly: H_2 and CO_2 during the positive polarization and H_2, CO, CO_2 and C_{2s} ($C_2H_4 + C_2H_6$) during the negative one. For both cases, after the polarizations the system returned to the initial OCV production rate values, demonstrating the reversibility of the polarization effect and the electrochemical nature of the different reaction processes. The effect of the polarizations could be explained attending to the electrochemical supplying of O^{2-} ions to the different electrodes during the polarizations. It is well known [26] that YSZ solid electrolyte behaves as a pure oxygen anion conductor material. Thus, considering the Pt film as the working electrode of the anionic solid electrolyte cell, and the Ag as the counter electrode, the application of positive currents led to the migration of O^{2-} ions from the Ag electrode to the Pt film through the YSZ solid electrolyte, and vice versa under the application of negative currents [27] (see Fig. 2). Hence, the application of a positive current of 200 mA (O^{2-} ions migrating from the Ag electrode to the Pt film) led to the reduction of steam in the Ag film (through a steam electrolysis process) to form hydrogen gas

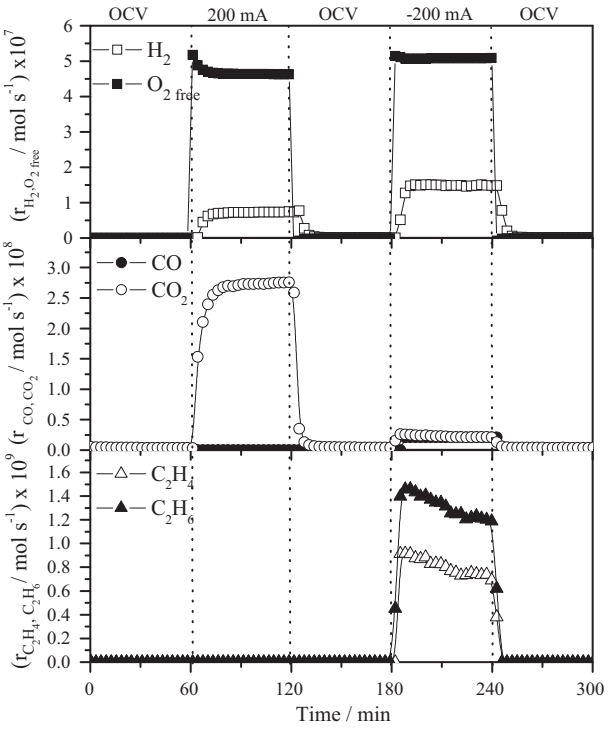

Fig. 1. Polarization and open circuit potential (OCV) effect on the dynamic value of H_2, $O_{2\,free}$, CO, CO_2, C_2H_6 and C_2H_4 reaction rates vs. time. Conditions: CH_4/H_2O: 1%/7%, total flow = 60 mL min^{-1} (N_2 balance), temperature = 750 °C.

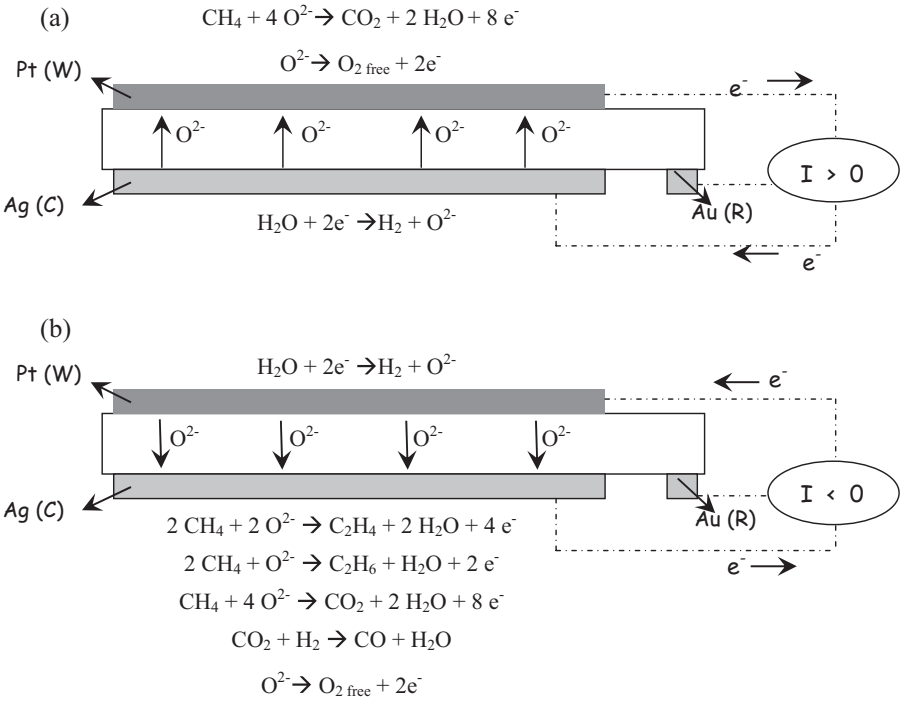

Fig. 2. Schematic representation of the main processes involved during the different polarizations.

and oxygen ions (O^{2-}) [28]. Then, H_2 released to the gas phase, and it was obtained as a reaction product, while O^{2-} ions were transported through the YSZ solid electrolyte to the Pt working electrode leading to the methane combustion reaction and hence to the production of CO_2 (Fig. 2a). No formation of CO and/or C_{2s} hydrocarbons was observed under these conditions, which can be attributed to the high activity of Pt for the combustion reactions vs. a possible coupling mechanism [29–31]. In this sense, although previous works [29–31] reported the syngas production from methane in an electrochemical membrane reactor based on Pt/YSZ, it should be noted that they worked under methane excess conditions, leading therefore to the electrocatalytic partial oxidation of methane instead of the deep oxidation process. However, the application of 200 mA in this experiment can be related to a CH_4/O_2 molar ratio of 0.79 (according to the Faradaic O^{2-} ions), and this can explain the main production of CO_2 observed in Fig. 1. On the other hand, it can be observed that the application of the negative current (−200 mA), led to the production of H_2, CO, CO_2 and C_{2s}. In this case, the application of this negative polarization led to the production of H_2 via steam electrolysis in the Pt film, while the electrochemically supplied O^{2-} ions led to the production of CO, CO_2 and C_{2s} hydrocarbons on the Ag counter electrode (as schematized in Fig. 2b). Regarding the observed CO production, this is not likely produced as a product of the coupling process in Ag electrodes. Previous works with double chamber SEMRs have not shown any CO production by electrochemical supplying of O^{2-} ions to a silver electrode [11,21,30]. Moreover, the partial oxidation of CH_4 can be neglected since Ag is not an active catalyst electrode for this process. Thus, the formation of CO under the application of a negative polarization was attributed to the CO_2 hydrogenation process, i.e., the reverse water gas shift reaction (RWGS) due to the presence of H_2 in the feed stream. Pekridis et al. [32] demonstrated the catalytic activity of a Pt electrode supported over YSZ in the RWGS at high temperatures (700–800 °C), reporting even the possibility of an electro-promotional effect under the application of negative polarizations, as in the case of the present study. This way, the results obtained under the application of the negative current are in good agreement with previous works which have demonstrated in a double chamber atmosphere the good performance of Pt electrodes towards the steam electrolysis process [33], and also the selectivity of Ag electrodes to the methane coupling reaction, with the subsequent formation of C_{2s} hydrocarbons [11,18,21,34]. On the other hand, Fig. 1a despites the variation of the free O_2 ($O_{2\,free}$) under the different current impositions. The ($O_{2\,free}$) represents the amount of O_2 coming from the electrolysis process which did not react with CH_4 to produce CO, CO_2, C_2H_4 and C_2H_6 and then can homogeneously react with the produced H_2, decreasing the Faradaic efficiency of the process. Then, to define this parameter, it was taken into account the non-reacted O^{2-} ions with the methane by means of the reactions depicted in Fig. 2b (methane combustion and coupling reactions). Hence, these non-reacted O^{2-} ions were recombined to form $O_{2\,free}$, which desorbed to the gas phase. Thus, since the theoretical O_2 flow can be calculated by means of the Faraday law, taking into account the oxygen consumption by the combustion and coupling reactions (see Fig. 2b), the free O_2 can be calculated by Eq. (5):

$$O_{2\,free} = \frac{I}{4 * F} - 2 * r_{CO_2} + r_{C_2H_4} + 0.5 * r_{C_2H_6} \quad (5)$$

Thus, Fig. 1a shows a slightly lower amount of free O_2 under the application of positive polarizations in comparison with negative ones. It could be attributed to a higher oxygen conversion towards the combustion products due to the high amount of CO_2 produced under these conditions. Very likely, this free O_2 could homogeneously react with H_2, decreasing therefore the apparent Faradaic efficiency (defined by Eq. (4)) of the experimentally measured H_2 (analyzed with the micro-GC). Hence, one could expect to obtain a higher H_2 production under the application of the positive current. However, this later polarization led to a lower H_2 reaction rate in comparison with the negative one in view of the results of Fig. 1. It could be attributed to the faster O_2 evolution in the Pt electrode respect to the Ag one. Hence, as it was explained by Tsiakaras and Vayenas [21], apart to the O_2 evolution in the silver layer, O^{2-} ions can desorbed to form Oxygen dissolved species (O_d) at the two phase boundary YSZ-Ag, being these later ones the active species in the reaction of oxidative coupling of methane.

Then, it seems that this latter negative polarization is of great interest since it allows to simultaneously produce C_{2s} hydrocarbons and H_2 for the first time in literature in an electrolysis cell. In this latter process an apparent Faradaic efficiency of 0.143 was calculated on the basis of Eq. (4). This low value could be attributed to the further reaction of H_2 with other molecules present in the single chamber atmosphere such as CO_2 or free O_2 (as already explained). This kind of sub-Faradaic efficiency is expected to occur in a single chamber steam electrolysis cell (where H_2 is not separated from the other molecules), but it could be compensated in this case by the simultaneous production of C_{2s} hydrocarbons.

One can find in literature a few number of studies for the simultaneous production of H_2 and C_{2s} hydrocarbons by using conventional catalytic reactors [35,36]. However, the performance of these systems is radically different to that shown in this work, following a combined concept which utilizes not only the CO_2 and steam provided by the oxidative coupling process for the reforming reaction, but also the exothermicity from the coupling reaction to support the steam reforming process [35], or by the combination of the homogeneous–heterogeneous methane partial oxidation with the coupling reactions [36]. On the other hand, several studies were carried out in SEMRs for the simultaneous production of H_2 and C_{2s} following the concept of a non-oxidative methane dehydrogenation assisted by a protonic solid electrolyte membrane. The solid state proton conductors were used to electrochemically pump out hydrogen from methane, leading to the simultaneous production and separation of hydrogen (in the case of double chamber reactors) and a mixture of ethane and ethylene [37–41]. However, low yields were reported (lower than 2%), probably since this process was strongly limited by the formation of carbon filaments in the absence of oxygen due to the methane cracking reaction [14], which led to the deactivation of the coupling electrode. However, the configuration used in this work provides a new concept which allows to in situ control the amount of the desired products by the current application, and on the other hand, to avoid the feeding of O_2 due to the use of an O^{2-} ion conductor solid electrolyte membrane (i.e., YSZ) as an oxygen supplier to the Ag coupling electrode. This configuration would also avoid the typical deactivation phenomena previously mentioned due to carbon deposition on the catalytic active sites due to both, the presence of steam in the feed stream, and the O^{2-} ions supplied through the YSZ solid electrolyte. Thus, considering that the production of C_{2s} hydrocarbons only occurred under the application of the negative current (O^{2-} ions electrochemically transferred to the Ag electrode), the rest of the experiments shown in this paper were performed under negative polarization mode (cathodic currents impositions).

Fig. 3 shows the dynamic response of the electrochemical cell for the production of H_2 (a), CO and CO_2 (b) and C_{2s} (c) under the application of different negative polarizations from −20 mA to −400 mA. Each negative polarization was carried out for 60 min and under the same experimental conditions (750 °C and CH_4/H_2O: 1%/7%, with a total flow rate of 60 mL min^{-1}). Fig. 3a shows an almost linear trend of H_2 production with the applied current, demonstrating, as previously mentioned, that obtained H_2 comes from the steam electrolysis process in the Pt film (negatively polarized) and no other catalytic contribution was observed under the explored conditions.

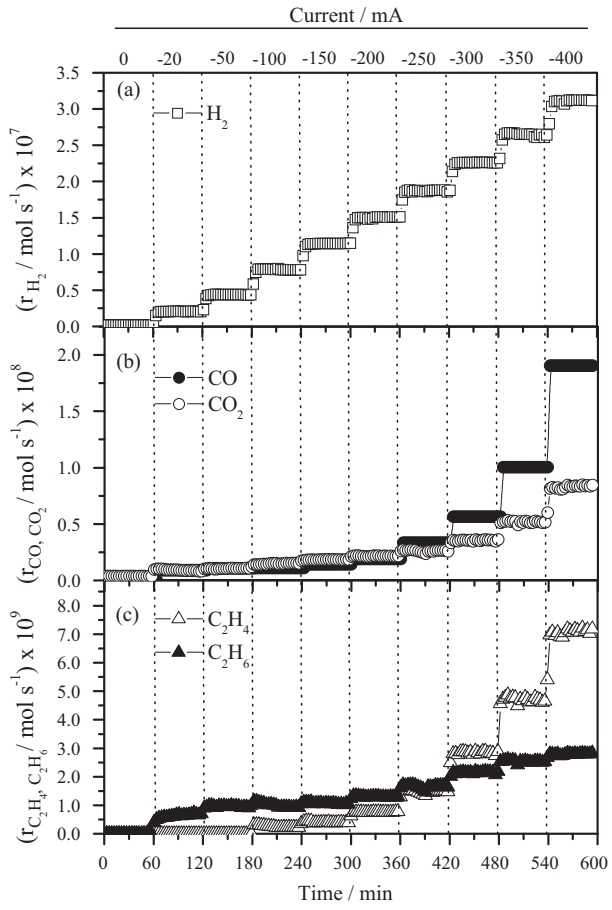

Fig. 3. Influence of the applied current on the dynamic value of H_2, CO, CO_2, C_2H_6 and C_2H_4 reaction rate vs. time. Conditions: CH_4/H_2O: 1%/7%, total flow = 60 mL min^{-1} (N_2 balance), temperature = 750 °C.

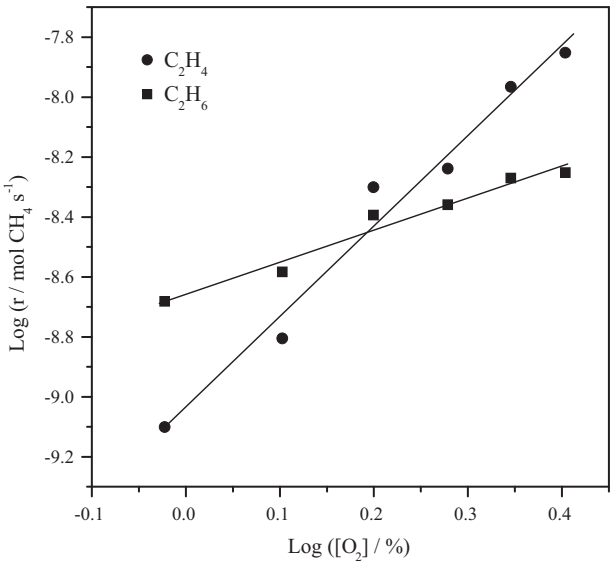

Fig. 4. Effect of O_2 concentration on the rates of formation of C_2H_4 and C_2H_6. Conditions: CH_4/H_2O: 1%/7%, total flow = 60 mL min^{-1} (N_2 balance), temperature = 750 °C.

Again, the average Faradaic efficiency obtained ($\Lambda = 0.145$) at all polarizations was lower than 1, which can be attributed, as already mentioned, to the partial recombination of H_2 and free O_2 present in the gas phase. On the other hand, it can also be observed an increase in the formation of carbon-derived products (CO, CO_2 and C_{2s}) with increasing the applied current. This effect is easy to understand considering that an increase in the applied cathodic current led to an increase in the amount of oxygen ions (O^{2-}) supplied to the Ag electrode, improving therefore the methane reaction rate, with the subsequent positive effect in the formation of CO, CO_2, C_2H_4 and C_2H_6. Again, as explained in Fig. 1, one could rule out the partial oxidation of CH_4 on the Ag electrode [11,21,30], being the most plausible origin of the observed CO the CO_2 hydrogenation reaction [32]. Hence, as the cathodic current increased, the amount of produced H_2 and CO_2 increased, which led to an increase in the CO_2 hydrogenation reaction with the subsequent increase in the CO production rate. Fig. 3c shows the variation of ethane and ethylene production with time and current. In this figure it can be observed that both C_{2s} production rates increased with the applied current. However, a different trend of these products (ethane and ethylene) could be observed. Below -200 mA, ethane was the main C_2 product, while at more negative cathodic currents the ethylene production was predominant. This trend can be better explained by looking at Fig. 4, which shows the steady state kinetic data of the C_{2s} products respect to the gas phase O_2 concentration (i.e., equivalent O_2 flow electrochemically supplied to the Ag electrode and calculated on the basis of the applied current [11]). Then, in this figure it can be observed the significantly higher reaction order of ethylene vs. ethane formation, which suggests that C_2H_4 is a secondary reaction product resulting from the Oxidative Dehydrogenation of Ethane (ODE from now on), in good agreement with a previous work by Tsiakaras and Vayenas [21]. This conclusion is also in good agreement with the obtained results shown in Fig. 3c, where C_2H_4 was formed under the application of the highest negative currents and once the ethane concentration attained certain value. Several authors have made an effort to clarify the homogeneous pathways of the ODE process [42–45]. Thus, they observed an important contribution of the ODE homogeneous reaction at temperatures higher than 700 °C, being ethylene and CO the main products (the former with a selectivity higher than 60%). Also, Mulla et al. [45] studied the influence of the introduction of steam in the feed stream, and they did not find an important variation of the ethane conversion and the products selectivity in a wide range of temperatures. Then, it seems to indicate that the combination of the heterogeneous and homogeneous pathways led to the production of ethane by the electrocatalytic activity of Ag towards the methane oxidative coupling, whereas the homogeneous gas phase reaction (ODE) would lead to the production of the ethylene. Nevertheless, a very small amount of C_2H_4 may be also directly formed as an initial reaction product of the methane coupling reaction [46].

3.2. Influence of the working temperature

Fig. 5 depicts the variation of the steady state H_2 (a), CH_4 (b) and $O_{2\,free}$ (c) reaction rates as a function of the applied current (and the equivalent O_2 flow electrochemically supplied to the Ag electrode, in the secondary abscissa axis) for different reaction temperatures (750 °C, 790 °C and 820 °C), under the same composition of the previous experiments. Firstly it was observed, for all the studied temperatures, an almost linear increase of the H_2 production rate with the current. As explained above, it can be mainly attributed to the steam electrolysis process in the Pt electrode. In addition from Fig. 5a it can be observed that the higher the reaction temperature, the higher the production of H_2. Hence, an increase in the average apparent Faradaic efficiency can be calculated at higher temperatures, i.e., $\Lambda = 0.145$, 0.151 and 0.186 at $T = 750$ °C, 790 °C and 820 °C, respectively. In this sense, one can think that the H_2 production could be enhanced from the following processes: methane steam reforming, methane partial oxidation and C_{2s} reforming. The first one can be neglected since catalytic activity

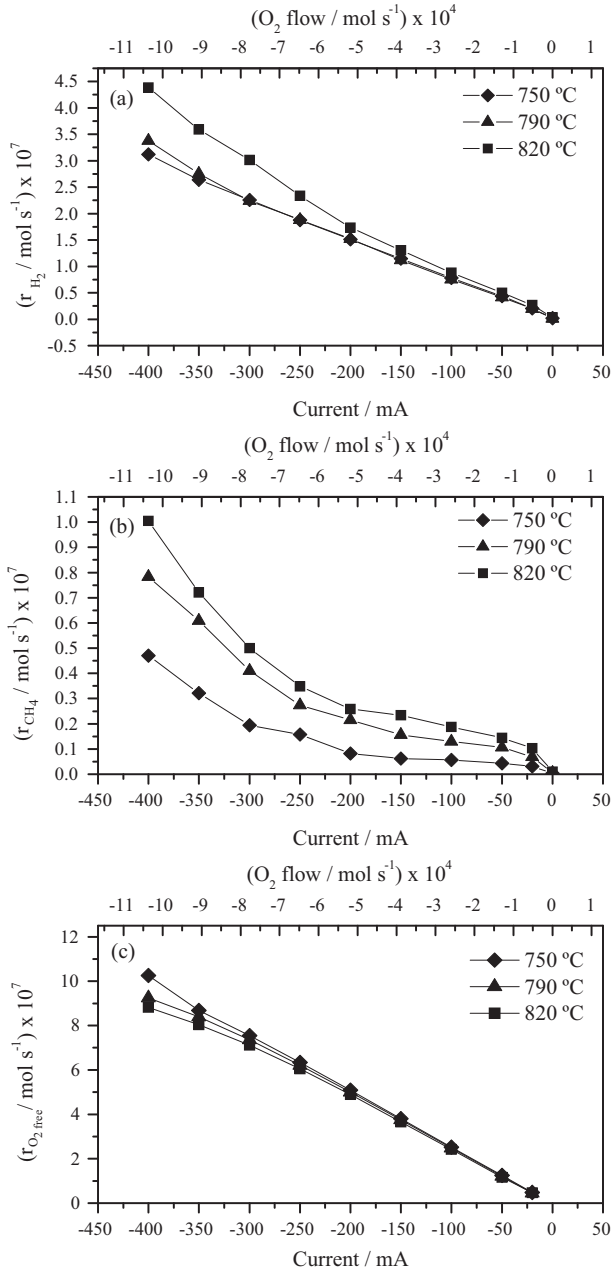

Fig. 5. Influence of the reaction temperature, current imposition and equivalent flow of O_2 supplied on the H_2, CH_4, $O_{2\,free}$ reaction rates. Conditions: CH_4/H_2O: 1%/7%, total flow = 60 mL min^{-1} (N_2 balance).

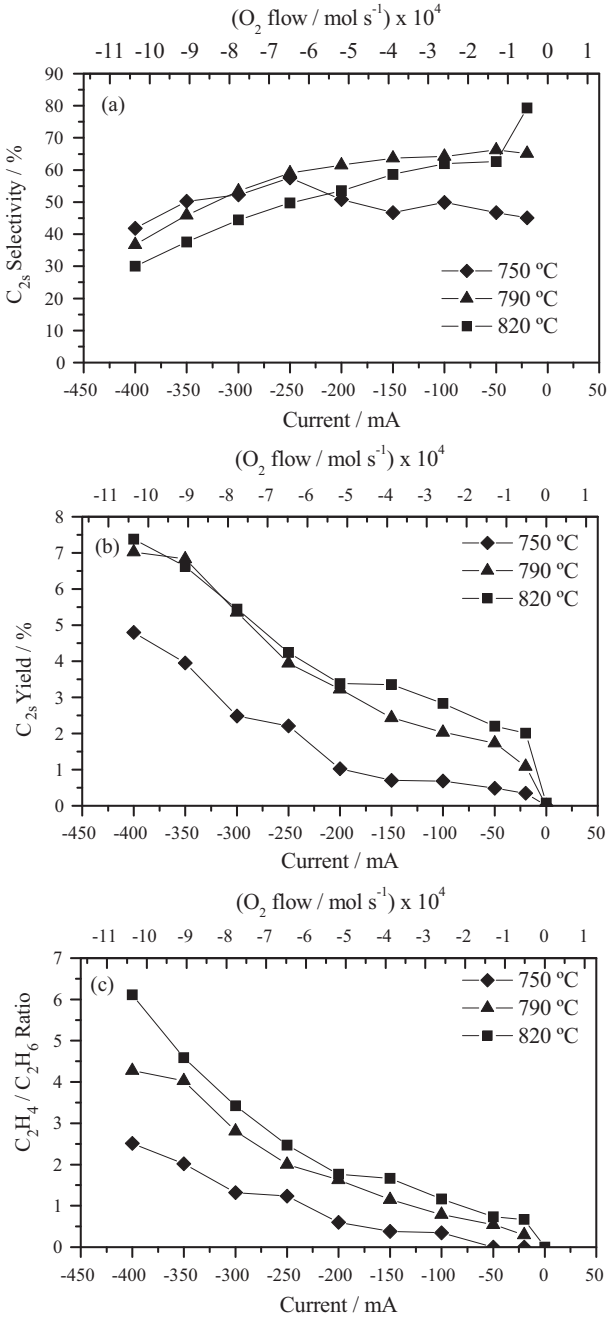

Fig. 6. Influence of the reaction temperature, current imposition and equivalent flow of O_2 supplied on the C_{2s} selectivity (a), C_{2s} yield (b) and C_2H_4/C_2H_6 ratio (c). Conditions: CH_4/H_2O: 1%/7%, total flow = 60 mL min^{-1} (N_2 balance).

was not observed under OCV conditions ($I = 0$). Regarding the catalytic activity towards the methane partial oxidation, no important CO production was observed in studies with similar Ag electrode at temperatures up to 850 °C [11,21,30], being CO_2 and C_{2s} the main observed products. This indicates again that the high CO production observed probably was produced via CO_2 hydrogenation. Finally, the C_{2s} reforming reaction can be also neglected, since the amount of C_{2s} produced in the temperature window studied in this work was around two orders of magnitude lower than that coming from the H_2 production rate. Hence, one can explain the slightly increase in the efficiency of the system to produce H_2 at higher temperatures on the basis of the lower free O_2 in the single chamber gas atmosphere (Fig. 5c). Thus, one can observe a similar trend of the CH_4 reaction rate (Fig. 5b) increasing with both, the applied current and the applied potential. As already mentioned, an important part of the H_2 produced through the electrolysis process was recombined with free O_2 to produce H_2O, leading to apparent Faradaic efficiencies lower than 1. However, as the reaction temperature increased the amount of free O_2 in the gas phase decreased (Fig. 5c), since a higher amount of it react with CH_4, via combustion and/or oxidative coupling mechanism, i.e., the CH_4 conversion increased with the reaction temperature (Fig. 5b). On the other hand, Fig. 6 displays the C_{2s} production corresponding to the same experiment shown in Fig. 5, showing the variation of the C_{2s} selectivity (Fig. 6a), the C_{2s} yield (Fig. 6b) and the C_2H_4/C_2H_6 ratio (Fig. 6c). Then, in Fig. 6a it can be observed a low variation of the C_{2s} selectivity with the applied current at 750 °C. However, at 790 °C and 820 °C, a general decrease of the selectivity was observed with increasing the amount of supplied electrochemical oxygen. It could be

attributed to the competition of the complete oxidation reaction, i.e., combustion, of both, CH_4 and C_{2s} products, with the growing supplied O_2 amount at higher cathodic currents [11]. Thus, according to previous studies with conventional heterogeneous catalysts [47], it is generally accepted that the OCM reaction involves, in a first step, the generation of methyl radicals, in which oxygen species are strongly involved. Then, they would combine to form the desired C_2 species by the heterogeneous-homogeneous pathways described above. However, as was reported by Lapeña-Rey [11], the further oxidation of these methyl radicals competes with the desired coupling reaction, leading to the production of CO_2 and therefore limiting the C_2 selectivity. Thus, when the amount of oxygen present in the reaction atmosphere exceeds the relatively low amount required to form a methyl radical, the competition between deep oxidation and coupling reaction increases (decreasing C_{2s} selectivity). In addition, once the C_2 hydrocarbons are formed, the possibility of their further oxidation (combustion) increases with the O_2 concentration (free O_2 desorbed to the gas phase from non reacted O^{2-} ions), which would also explain the decrease in the C_{2s} selectivity at stronger cathodic currents. On the other hand, the C_{2s} yield variation showed a continuous increase with both, the applied current and the reaction temperature, leading to a maximum C_{2s} yield of 7.5% at 820 °C (Fig. 6b). These results are in good agreement with the trends observed in the aforementioned study [11] using a double chamber configuration with an approximate similar maximum C_{2s} yield value. Hence, as the amount of O_2 electrochemically supplied to the Ag electrode increased (higher cathodic currents), the ratio of the coupling vs. the combustion reaction decreased (lower C_{2s} selectivity) but the overall C_{2s} yield increases, therefore leading to a higher amount of C_{2s}. On the other hand, it should be mentioned that the possibility of the simultaneous production of H_2 in the present work, i.e., 4.4×10^{-7} mol s^{-1} under the optimal C_{2s} yield production of 7.5%, increased the overall economic efficiency of the system. In other words, under the same applied current (i.e., under the same consumed power), both kind of products (H_2 and C_{2s}) could be simultaneously produced. Finally, the trend of the C_2H_4/C_2H_6 ratio with the applied current was depicted in Fig. 6c. It can also be observed a general increase of this ratio with the cathodic current and the reaction temperature and, hence in the production of the desired hydrocarbon (ethylene). These results are again in good qualitative agreement with the heterogeneous-homogeneous pathways related with the ODE reaction (Figs. 3 and 4), since an increase in the reaction temperature probably led to an enhancement of the gas phase steps for this reaction, therefore increasing the ratio between the ethylene and ethane. On the other hand, it seems that the increase in the oxygen supplied to the Ag electrode enhanced the ODE reaction, probably due to the participation of oxygen in the dehydrogenation steps [42], leading to a higher production of C_2H_4 vs. C_2H_6.

3.3. Influence of the composition

In order to study the influence of the composition (CH_4/H_2O ratio in the feed), it was carried out a sequence of experiments under a constant applied current (equivalent to a constant oxygen flow) and at constant steam concentration (7%), by varying the methane concentration in the feed stream (0.3–1.3%) at a temperature of 820 °C. Then, Fig. 7a–d shows the variation of the steady state H_2, CH_4, $CO + CO_2$ and $C_2H_4 + C_2H_6$ reaction rates, respectively, with the feed methane concentration under the application of three constant currents: −250 mA, −300 mA and −350 mA. It can be observed that the H_2 production rate had the same trend as the CH_4 reaction rate, and attained a maximum value at a certain CH_4 inlet concentration (denoted as CH_4^{opt}) which depended on the applied current. These results demonstrated again that the H_2 production strongly depends on the free gas phase O_2 (not combined with CH_4). Hence,

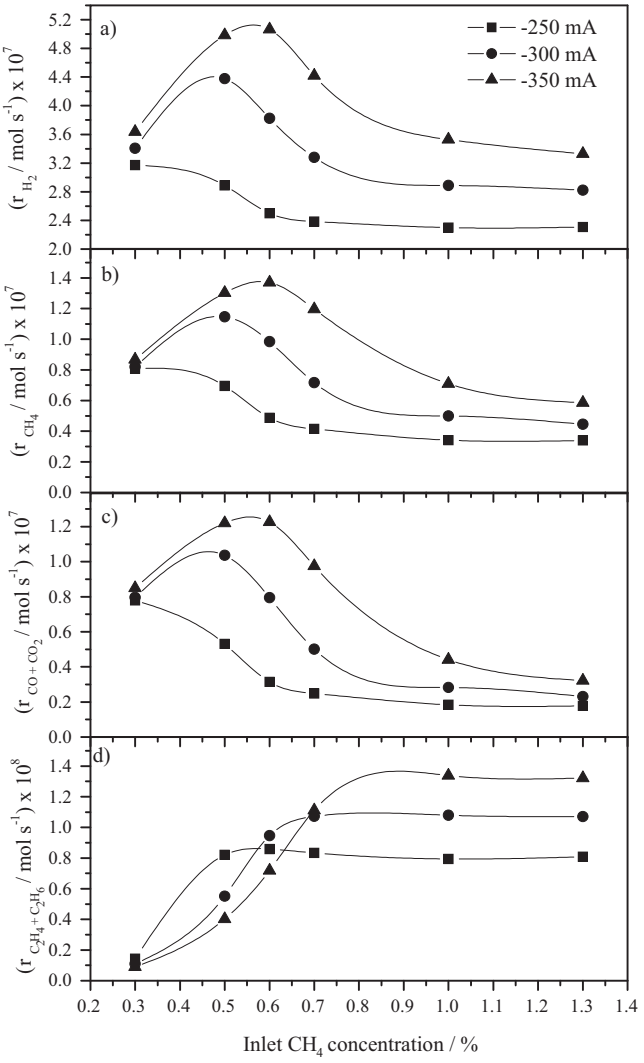

Fig. 7. Influence of the inlet CH_4 concentration at different current impositions on the H_2, CH_4, $CO + CO_2$ and $C_2H_4 + C_2H_6$ reaction rates. Conditions: CH_4/H_2O: 0.3–1.3%/7%, total flow = 60 mL min^{-1} (N_2 balance), temperature = 820 °C.

although at higher negative currents, the H_2 produced by the steam electrolysis process increased (mol_{H_2} $s^{-1} = I/2F$), the final experimentally measured H_2 also depended on the free O_2 not reacted with CH_4. At a CH_4 concentration higher than CH_4^{opt} (CH_4 concentration at which the CH_4 reaction rate attained a maximum), the free O_2 in the gas phase started to increase, which led to the overall decrease in the production of H_2. At this point it should be mentioned that the appearance of a maximum in the CH_4 conversion is due to the kinetics of the CH_4 combustion reaction (i.e., CH_4 reaction rate followed the same trend as the $CO + CO_2$ reaction rate, being CO the major product probably due to the CO_2 hydrogenation process, as mentioned above). Hence, there was an optimum CH_4 coverage which maximized the combustion reaction, and which depended on the amount of O^{2-} (applied current). Thus, an increase in the amount of O^{2-} supplied to the Ag electrode (higher cathodic current) led to a higher CH_4^{opt}, i.e., the maximum CH_4 combustion rate was attained at higher CH_4 inlet composition. Hence, one can calculate an average optimum CH_4/O_2 coverage ratio of 0.24 for the three studied currents. On the other hand, it can be observed that above the CH_4^{opt} value, the oxidative coupling reaction started to compete with the CH_4 deep oxidation, leading to a growing production of C_{2s}. As already mentioned, the oxygen species are strongly involved in the generation of the starting methyl radicals. However,

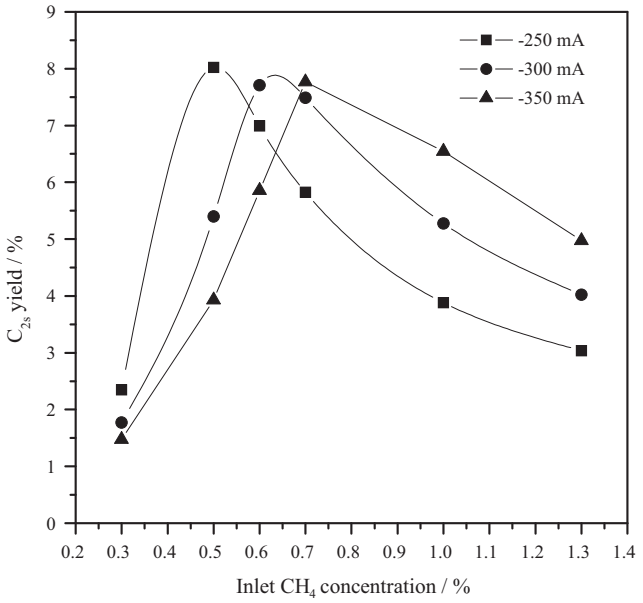

Fig. 8. Influence of the inlet CH_4 concentration at different current impositions on the C_{2s} yield. Conditions: CH_4/H_2O: 0.3–1.3%/7%, total flow = 60 mL min^{-1} (N_2 balance), temperature = 820 °C.

when the oxygen content was higher than the amount necessary to form a methyl radical, the competition between deep oxidation and methane coupling reaction increased. Summarizing, at low methane concentrations (which correspond with a low methane to oxygen ratio), the methane combustion is the main process, whereas at higher methane to oxygen ratios the catalytic activity towards the C_{2s} production was enhanced.

Fig. 8 depicts the variation of the C_{2s} yield with the methane concentration at the different studied currents. Thus, in this figure it can be observed an optimum value of C_{2s} yield of around 8% at each polarization. However, the methane concentration at which this optimum was attained varied on the basis of the applied current. Then, the higher the applied current, the higher the methane concentration necessary in the feed stream to reach the maximum yield value. It implies also that there is an optimum CH_4/O_2 coverage ratio for the formation and further evolution of the methyl radicals for the production of C_{2s} hydrocarbons. Hence, one can calculate an optimum CH_4/O_2 ratio value of 0.31 for the three cathodic polarizations. Then, the use of the solid electrolyte cell allows by simply adjusting the applied current to achieve this optimum coverage at varying reaction conditions, i.e., the reaction temperature and/or CH_4 concentration in the feed, according to the explanations given above. This fact would justify that in Fig. 6 it was not achieved a maximum value of C_{2s} yield at the same reaction temperature (820 °C), since the optimum CH_4/O_2 ratio (0.31) would be reached under the application of −500 mA at the methane feed stream concentration of 1%. On the other hand, it should be mentioned that, according to the discussion made in Fig. 7, the optimum ratio for the C_{2s} yield (0.31) is close to that found for the CH_4 conversion of 0.24 (and hence for the H_2 production via single chamber steam electrolysis). Then, for the practical application of this configuration, one can anticipate the optimum current working conditions which led to a CH_4/O_2 ratio between 0.24 and 0.31, where the production rate of the main products (H_2 and C_{2s}) can be maximized.

3.4. Durability study

Finally, a long durability study under the optimal reaction conditions obtained in Fig. 7, at 820 °C regarding the C_{2s} yield was carried out (I = −350 mA, $[CH_4]/[H_2O]$: 0.7%/7%). Thus, Fig. 9 shows the variation of the reaction rates of the obtained products during 18 h. A suitable activity and stability under the explored reaction conditions was observed, showing a high potential for the practical development of this system. Nevertheless, further research work should be done in order to improve the performance of the proposed novel configuration (single chamber cell) using the same concept. For instance, the use of a double chamber atmosphere or the use of more selective electrodes. The use of a double chamber configuration will allow to produce pure H_2 with 100% of efficiency and without interaction with other molecules. The use and development of more selective electrodes instead of Ag would allow to increase the yield and the selectivity of the C_{2s} hydrocarbons.

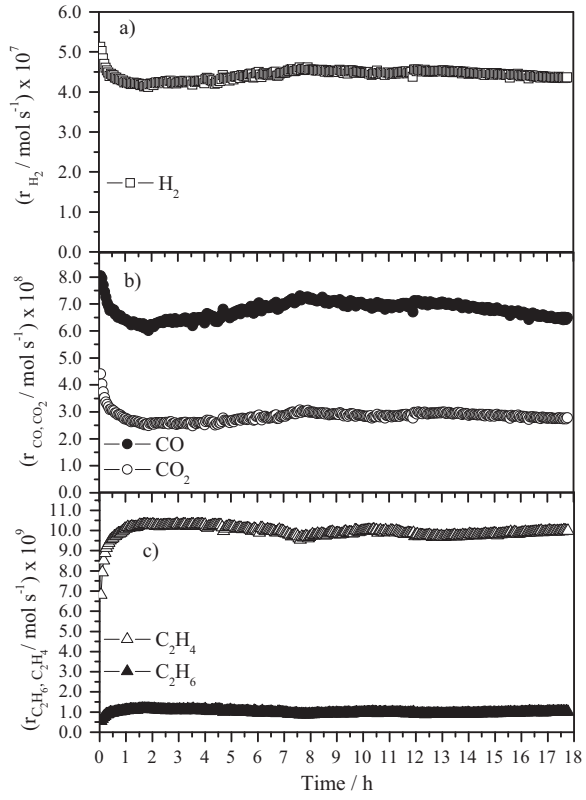

Fig. 9. Variation of the H_2, CO, CO_2, C_2H_6 and C_2H_4 reaction rates with time during a durability study. Conditions: CH_4/H_2O: 0.7%/7%, total flow = 60 mL min^{-1} (N_2 balance), temperature = 820 °C, current = −350 mA.

4. Conclusions

A new concept which integrates a single chamber electrolysis cell for the production of H_2 and the simultaneous production of C_{2s} hydrocarbons has been introduced and developed in this work. The proposed single chamber cell Pt/YSZ/Ag has been investigated under CH_4/H_2O atmosphere under different reaction conditions. Different conclusions of great importance can be obtained from this work:

- The application of negative currents allows to simultaneously produce both kind of products H_2 and C_{2s} hydrocarbons.
- The H_2 production rate and C_{2s} yield was enhanced by stronger applied cathodic polarizations and by an increase in the reaction temperature.
- For the simultaneous production of H_2 and C_{2s}, an optimum current range was found, corresponding to the equivalent O_2 flow

electrochemically supplied to the Ag electrode and calculated on the basis of the applied current by I/4F.
- The developed single chamber cell has shown to be stable for long working polarization times and hence shows potential for its further practical application.

Acknowledgment

We gratefully acknowledge Spanish MICINN projects CTQ 2007-62512/PPQ, CTQ 2008-02940-E (corresponding to ACENET ERA-NET project, ACE.07.016).

References

[1] B.D. McNutt, L.R. Johnson, Competing against entrenched technology: implications for U.S. government policies and fuel cell development, in: Presented at the Pre-Symposium Workshop of the Sixth Grove Fuel Cell Symposium, London, UK, 1999.
[2] J.D. Holladay, J. Hu, D.L. King, Y. Wang, Catal. Today 139 (2009) 244–260.
[3] M.A. Peña, J.P. Gomez, J.L.G. Fierro, Appl. Catal. A 144 (1996) 7–57.
[4] J.N. Armor, Appl. Catal. A 176 (1999) 159–176.
[5] A.J. Esswein, D.G. Nocera, Chem. Rev. 107 (2007) 4022–4047.
[6] D.R. Palo, R.A. Dagle, J.D. Holladay, Chem. Rev. 107 (2007) 3992–4021.
[7] M. Ni, D.Y.C. Leung, M.K.H. Leung, Int J. Hydrogen Energy 32 (2007) 3238–3247.
[8] P.K. Cheekatamarla, C.M. Finnerty, J. Power Sources 160 (2006) 490–499.
[9] X-M. Guo, K. Hidajat, C-B. Ching, Ind. Eng. Chem. Res. 36 (1997) 3576–3582.
[10] G.E. Keller, M.M. Bhasin, J. Catal. 73 (1982) 9–19.
[11] N. Lapeña-Rey, P.H. Middleton, Appl. Catal. A 240 (2003) 207–222.
[12] V.R. Choudhary, B.S. Uphade, Catal. Surv. Asia 8 (2004) 15–25.
[13] I. Garagounis, V. Kyriakou, C. Anagnostou, V. Bourganis, I. Papachristou, M. Stoukides, Ind. Eng. Chem. Res. 50 (2011) 431–472.
[14] M. Stoukides, Res. Chem. Int. 32 (2006) 187–204.
[15] M. Stoukides, Catal. Rev. Sci. Eng. 42 (2000) 1–70.
[16] C. Kokkofitis, M. Ouzounidou, A. Skodra, M. Stoukides, Solid State Ionics 178 (2007) 507–513.
[17] M. Stoukides, Ind. Eng. Chem. Res. 27 (1988) 1745–1750.
[18] K. Otsuka, S. Yokoyama, A. Morikawa, Chem. Lett. 14 (1985) 319–322.
[19] K. Otsuka, K. Suga, I. Yamanaka, Catal. Lett. 1 (1988) 423–428.
[20] C.G. Vayenas, S. Bebelis, I.V. Yentekakis, H.-G. Lintz, Catal. Today 11 (1992) 303–438.
[21] P. Tsiakaras, C.G. Vayenas, J. Catal. 144 (1993) 333–347.
[22] Y. Jiang, I.V. Yentekakis, C.G. Vayenas, Science 264 (1994) 1563–1566.
[23] J. Martinez-Frias, A-Q. Pham, S.M. Aceves, Int J. Hydrogen Energy 28 (2003) 483–490.
[24] A. de Lucas-Consuegra, A. Caravaca, P.J. Martínez, J.L. Endrino, F. Dorado, J.L. Valverde, J. Catal. 274 (2010) 251–258.
[25] F. Dorado, A. de Lucas-Consuegra, P. Vernoux, J.L. Valverde, Appl. Catal. B 73 (2007) 42–50.
[26] L. Malavasi, C.A.J. Fisherb, M. Saiful Islam, Chem. Soc. Rev. 39 (2010) 4370–4387.
[27] C.G. Vayenas, S. Bebelis, C. Pliangos, S. Brosda, D. Tsiplakides, Electrochemical Activation of Catalysis: Promotion, Electrochemical Promotion and Metal-Support Interactions, Kluwer Academic Publishers/Plenum Press, New York, 2001.
[28] M. Ni, M.K.H. Leung, D.Y.C. Leung, Int. J. Hydrogen Energy 33 (2008) 2337–2354.
[29] G.L Semin, V.D. Belyaev, A.K. Demin, V.A. Sobyanin, Appl. Catal. A 181 (1999) 131–137.
[30] V.A. Sobyanin, V.D. Belyaev, V.V. Gal′vita, Catal. Today 42 (1998) 337–340.
[31] V.V. Gal′vita, V.D. Belyaev, V.N. Parmon, V.A. Sobyanin, Catal. Lett. 39 (1996) 209–211.
[32] G. Pekridis, K. Kalimeri, N. Kaklidis, E. Vakoufsi, E.F. Iliopoulou, C. Athanasiou, G.E. Marnellos, Catal. Today 127 (2007) 337–346.
[33] T. Ishihara, T. Kannou, Solid State Ionics, in press.
[34] A.G. Anshits, A.N. Shigapov, S.N. Vereshchagin, V.N. Shevnin, Catal. Today 6 (1990) 593–600.
[35] S. Ren, S. Qin, J. Zhu, X. Peng, C. Hu, Ind. Eng. Chem. Res 49 (2010) 2078–2083.
[36] H. Zhang, J. Wu, B. Xu, C. Hu, Catal. Lett. 106 (2006) 161–165.
[37] K. Mori, JP Patent 62-240777 (1987).
[38] P.-H. Chiang, D. Eng, M. Stoukides, J. Electrochem. Soc. 138 (1991) L11–L12.
[39] P.-H. Chiang, D. Eng, M. Stoukides, Catal. J. 139 (1993) 683–687.
[40] L.S. Woldman, V.D. Sokolovskii, Catal. Lett. 8 (1991) 61–66.
[41] P.-H. Chiang, D. Eng, H. Alqahtany, M. Stoukides, Solid State Ionics 53–56 (1992) 135–141.
[42] V.R. Choudhary, S.A.R. Mulla, AIChE J. 43 (1997) 1545–1550.
[43] Z.-S. Chao, E. Ruckenstein, J. Catal. 222 (2004) 17–31.
[44] E. Heracleous, A.A. Lemonidou, Appl. Catal. A: Gen. 269 (2004) 123–135.
[45] S.A.R. Mulla, O.V. Buyevskaya, M. Baerns, Appl. Catal. A: Gen. 226 (2002) 73–78.
[46] S. Pak, P. Qiu, J.H. Lunsford, J. Catal. 179 (1998) 222–230.
[47] K.D. Campbell, J.H. Lunsford, J. Phys. Chem. 92 (1988) 5792–5796.